Int J Adv Manuf Technol (1999) 15:863–868

The International Journal of
Advanced
Manufacturing
Technology

Physical Simulation of the Deflection in Turning of Thin Disk-Shaped Workpieces

E. Cheung[1], W. Yuan[2] and M. Hua[1]

[1]Department of Manufacturing Engineering and Engineering Management, City University of Hong Kong, Kowloon, Hong Kong; and
[2]Institute of Computer Integrated Manufacturing System, Northwestern Polytechnical University, Xi'an, PR China

The machining of a thin disk-shaped workpiece is a problem commonly encountered in the aeronautics industry. Generally, the successful machining of a thin disk requires reinforcement by plaster. This reduces the productivity and increases the production cost. It is recognised that the suitable control of the cutting force to limit the maximum deflection of the disk within a certain value for each loading allows the machining to be successfully carried out without any plaster reinforcement. Modelling and computer-simulation of the deflection of a thin disk-shaped workpiece during turning are thus developed. The results of the simulation are discussed.

Keywords: Computer-aided simulation; Thin disk deflection; Thin disk machining; Turning

1. Introduction

Most thin disk-components used in the aeronautical industry are difficult to machine because of their small flexural rigidity for resisting the cutting force exerted. Although there are a number of techniques available for successful machining of such disks, they are inefficient and costly. The typical turning procedure for such components is, first, to fill the hollow parts of the disks with plaster, on the side which is not going to be machined, then the plaster-reinforced disk is clamped onto a turning fixture. The reinforcing plaster is taken off after turning. This method is time consuming and usually jeopardises productivity. Furthermore, the removal of the filling plaster may create problems of dimensional accuracy. Although the use of fixtures which support thin sections is also a common and preferred method to solve such turning problems, the production and mounting of fixtures are normally time consuming and costly. Additionally, one type of fixture can only be used for turning one kind of disk-shaped workpiece. Wastage of materials may occur if the fixtures are scrapped when they are thought to be no longer required or when there is no space to store them. Another solution to such difficult machining problems is to work out the turning conditions which provide a minimum and acceptable deflection profile by trial cuts, but, such an approach demands trial cuts to be undertaken for each material and each thickness. It is labour-exhaustive and wasteful of material. Also, the disk may be scrapped if it was carelessly machined. Additionally, it requires a highly skilled machinest to perform the task. Consequently, these types of thin disks are very costly to produce and accuracy is hard to maintain. The advance of computer simulation techniques provides the means to solve such machining problems by a series of simulations, visualisations and analyses [1–6]. Simulation of this kind can be classified into:

1. Geometrical simulation.
2. Physical simulation.

Geometric simulation predicts cutting kinematics controlling the movement of a cutter on the basis of multiple minimal-depth-feed allowable cuts within the NC programs [1–5]. It does not take into account of the cutting kinetics. Consequently, it cannot optimise the turning process, and may sometimes cause turning failure when the last step of an estimated cut exceeds the allowable stress for the thin disk. Consequently, scrapping may frequently occur. Realising this shortcoming of the geometric simulation, physical simulation to take account of cutting force and torque, cutting heat generation, disk deflection, and so on, is proposed [1,6] so as to optimise the machining phase of production. Because of the complexity of modelling the physical aspects in the machining stage, most researches in this field have been restricted to the geometric aspect [1–5]. Additionally, the current integration of virtual manufacturing technology with computer-aided simulation has the great merit of encouraging the development of virtual reality techniques [7].

The authors envisage that a physical simulation of the successful turning of a thin disk is possible if the maximum deflection, due to the application of cutting force, can be controlled to a level such that the deflection is within the allowable turning tolerance. With this in mind, this paper

Correspondence and offprint requests to: E. Cheung, Department of Manufacturing Engineering and Engineering Management, City University of Hong Kong, 83 Tat Chee Avenue, Kowloon, Hong Kong. E-mail: meedche@cityu.edu.hk

offers a methodology of physical simulation for analysing the deflection of a thin disk-shaped workpiece in turning. To demonstrate the validity of the simulation the deflection behaviour can be displayed, and the optimal parameters for the turning using virtual reality technology can be obtained. Furthermore, the simulation provides data for the selection of a turning sequence.

2. Mathematical Model of Thin Disk Deflection

A thin-walled part generally has an aspect ratio of thickness to minimum surface area between 1/100 and 1/8. Figure 1 shows this kind of disk which is loaded with a cutting force by a cutting tool on its turning face. Generally, the cutting load on the disk can be resolved into a component parallel to and another component perpendicular to the neutral plane of the disk. The perpendicular component will deflect the thin disk and it should be suitably controlled within the allowable limits.

2.1 Equation of Elastic Deflection Surface

Since the loaded disk is so thin, its deflection can be simulated as a loaded sheet disk under bending conditions. It is suggested that the machining can be successfully carried out if the maximum turning tolerance of the thin disk is smaller than the maximum deflection of a sheet disk deflected by the perpendicular component of the cutting force. In order to analyse such a turning problem it is further postulated that:

1. The shear strains, γ_{xz} and γ_{yz}, in the neutral plane of the bent sheet are zero throughout.
2. The displacements, i.e. u and v, in the neutral plane along the x- and y-directions (Fig. 1) are negligible when compared with the deflection w in the z-direction.
3. The stress σ_z perpendicular to the neutral plane is zero and the strain in the z-direction $\epsilon_z = 0$.

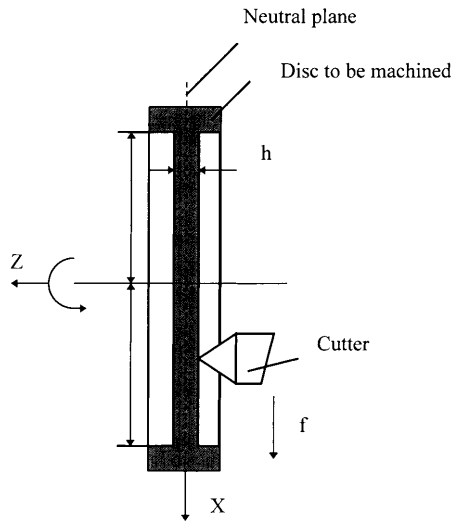

Fig. 1. Configuration of a thin disk during turning.

The postulation (1) thus gives [8–10]:

$$\gamma_{xz} = \frac{\partial u}{\partial z} + \frac{\partial w}{\partial x} = 0; \quad \gamma_{yz} = \frac{\partial w}{\partial y} + \frac{\partial v}{\partial z} = 0 \tag{1}$$

Integrating Eq. (1) with respect to z, we obtain:

$$u = -\frac{\partial w}{\partial x} z + f_1(x, y); \quad v = -\frac{\partial w}{\partial y} z + f_2(x, y) \tag{2}$$

From Eq. (2), it is reasonable to take $f_1(x, y) = f_2(x, y) = 0$. Therefore, the three strain components, i.e. ϵ_x, ϵ_y and γ_{xy}, in the (x, y)-plane can be expressed as a function of those relevant geometrical deflection profiles as:

$$\epsilon_x = \frac{\partial u}{\partial x} = -z\frac{\partial^2 w}{\partial x^2}, \quad \epsilon_y = \frac{\partial v}{\partial y} = -z\frac{\partial^2 w}{\partial y^2}, \quad \gamma_{xy} = \frac{\partial u}{\partial y} + \frac{\partial v}{\partial x} = -2z\frac{\partial^2 w}{\partial x \partial y} \tag{3}$$

respectively. Furthermore, Eq. (3) enables the establishment of the following physical equations.

$$\sigma_x = \frac{E}{1-\mu^2}(\epsilon_x + \mu\epsilon_y), \quad \sigma_y = \frac{E}{1-\mu^2}(\epsilon_y + \mu\epsilon_x) \tag{4a}$$

in which μ is the material Poisson's ratio and E is the Young's modulus of the workpiece. Substituting the geometrical equation (3) into the physical equation (4*a*), then further substituting the physical equation into the following equilibrium equation for a 3D element [11]:

$$\frac{\partial \sigma_x}{\partial x} + \frac{\partial \tau_{xy}}{\partial y} + \frac{\partial \tau_{xz}}{\partial z} = 0, \quad \frac{\partial \tau_{yx}}{\partial x} + \frac{\partial \sigma_y}{\partial y} + \frac{\partial \tau_{yz}}{\partial z} = 0, \quad \frac{\partial \tau_{zx}}{\partial x} + \frac{\partial \tau_{zy}}{\partial y} + \frac{\partial \sigma_z}{\partial z} = 0 \tag{4b}$$

then gives, after integration, the relevant stress functions as:

$$\tau_{zx} = \frac{Ez^2}{2(1-\mu^2)}\frac{\partial}{\partial x}\Delta^2 w + F_1(x, y), \quad \tau_{zy} = \frac{Ez^2}{2(1-\mu^2)}\frac{\partial}{\partial y}\Delta^2 w + F_2(x, y) \tag{5}$$

Since the deflection function w is independent of z, the boundary conditions of $\tau_{zx} = \tau_{zy} = 0$ at $z = \pm h/2$ (Fig. 1) further allow $F_1(x, y)$ and $F_2(x, y)$ to be evaluated from Eq. (5) which itself can then be re-expressed as:

$$\tau_{zx} = \frac{E}{2(1-\mu^2)}\left(z^2 - \frac{h^2}{4}\right)\frac{\partial}{\partial x}\Delta^2 w, \quad \tau_{zy} = \frac{E}{2(1-\mu^2)}\left(z^2 - \frac{h^2}{4}\right)\frac{\partial}{\partial y}\Delta^2 w \tag{6}$$

Substituting Eq. (6) into the third expression in Eq. (4*b*) gives:

$$\frac{\partial \sigma_z}{\partial z} = \frac{E}{1(1-\mu^2)}\left(\frac{h^2}{4} - z^2\right)\Delta^4 w \tag{7}$$

The integration of Eq. (7) gives:

$$\sigma_z = -\frac{E}{2(1-\mu^2)}\left(\frac{h^2}{4}z - \frac{z^2}{3}\right)\Delta^4 w + F_3(x, y) \tag{8}$$

The consideration of the boundary condition of $(\sigma_z)_{z=h/2} = 0$ for Eq. (8) allows the function $F_3(x, y)$ to be derived, and subsequently Eq. (8) to be re-expressed as:

$$\sigma_z = \frac{Eh^3}{6(1-\mu^2)}\left(\frac{1}{2}-\frac{z}{h}\right)^2\left(1+\frac{z}{h}\right)\Delta^4 w \tag{9}$$

Further, considering the boundary condition of $(\sigma_z)_{z=-h/2} = q$ for Eq. (9) permits Eq. (9) to be finally expressed as:

$$\sigma_z = \frac{Eh^3}{12(1-\mu^2)}\Delta^4 w = q \tag{10}$$

Equation (10), together with the consideration of geometrical compatibility and stress equilibrium provides a partial differential equation for the deflection surface of a thin sheet with uniformly distributed loading q per unit surface to be written as:

$$\frac{\partial^4 w}{\partial x^4} + 2\frac{\partial^4 w}{\partial x^2 \partial y^2} + \frac{\partial^4 w}{\partial y^4} = \frac{q}{D} \tag{11}$$

in which the deflection stiffness D of the thin sheet is:

$$D = \frac{Eh^3}{12(1-\mu^2)} \tag{12}$$

To facilitate the derivation of the bending analysis of a disk-shaped workpiece with radius r, Eq. (11) can be rewritten in polar coordinate system through a suitable transformation of $x = r\cos\theta$ and $y = r\sin\theta$. It then gives:

$$\left(\frac{\partial^2}{\partial r^2}+\frac{1}{r}\frac{\partial}{\partial r}+\frac{1}{r^2}\frac{\partial^2}{\partial \theta^2}\right)\left(\frac{\partial^2 w}{\partial r^2}+\frac{1}{r}\frac{\partial w}{\partial r}+\frac{1}{r^2}\frac{\partial^2 w}{\partial \theta^2}\right) = \frac{q}{D} \tag{13}$$

2.2 Boundary Condition

The solution of the deflection function $w(r, \theta)$ in Eq. (13) should conform to the boundary conditions of the thin disk-shaped workpiece to be turned. Generally, workpieces used in the aeronautics industry have a thicker rim than their spoke-plate. The relatively rigid rim thus allows the reasonable assumption of a fixed boundary condition to be made (Fig. 1). Let the outer radius of the spoke-plate be $r = a$, the deflection function must satisfy a boundary condition of $(w)_{r=a} = 0$, $(\partial w/\partial r)_{r=a} = 0$. That means, in a (X, Y)-coordinate system, $w(x, y) = 0$, $\partial w/\partial x = 0$ and $\partial w/\partial y = 0$ whenever $x^2 + y^2 = a^2$.

2.3 Load on Workpiece

There are loads due to cutting force, residual stress and thermal stress produced by cutting heat, on a thin disk-shaped workpiece, and all these loads cause deflections in turning. For simplification, only the cutting force and the residual membrane stress will be considered in the analysis, since the deflections caused by thermal stresses in cutting are usually negligibly small.

2.3.1 The Cutting Force

During cutting, the workpiece will deflect in the z-direction (Fig. 1) owing to the action of the cutting force. In turning, the cutting force can normally be expressed as [11]:

$$F_z = KCa_p f^a \sin^{1-\alpha} K_r \tag{14}$$

where C is a material coefficient; a_p is the cutting depth; f is the feedrate of a cut; α is an exponential index; K_r is the cutting-edge angle of a cutter; and K is a constant. At any instant of cutting, the cutting force will be concentrated at the cutting location. Its contribution to q in Eq. (13) will be zero throughout the spoke-plate except at its action point, where its contribution to q will be F_z.

2.3.2 The Residual Stress

Prior to turning material off the surface, the whole spoke-plate is in a state of stress equilibrium. When material on one of its surfaces is removed during turning, the stress equilibrium is disturbed and it releases residual membrane stress in the turned surface. Such residual stress yields an equivalent deflection $w_0 = w_0(r)$ in the z-direction (Fig. 1) of the spoke-plate. Generally, the direction of deflection will be either in the same direction as the loading direction of the cutting force, when compressive residual force results, or it will be in the positive direction, when tensile residual stress is obtained. Owing to the thinning effect of the spoke-plate, the level of the resultant of residual membrane stress increases as turning proceeds. To simplify the analysis, the residual membrane stress, say q_0, is first assumed to be evenly distributed in the disk surface. Let M_0 be the equivalent bending moment which causes the same amount of deflection of the spoke-plate, having radius a, second moment of area I and thickness h, due to q_0. The consideration of zero stress in the non-turned surface of the spoke-plate allows such an equivalent bending moment M_0 to be expressed as [9] $M_0 = q_0 I/h$ when the disk is turned at r from its centre. Subsequently, the corresponding deflection is given as:

$$\frac{d^2 w_0(r)}{dr^2} = \frac{M_0}{EI} = \frac{q_0}{Eh} \tag{15}$$

Let q_0' be a visible normal stress on the disk surface, which generates the equivalent deflection $w_0 = w_0(r)$, as described by Eq. (15), its respective deflection in the disk will be [9]:

$$w_0(r) = \frac{12q_0'(1-\mu^2)}{64Eh^3}(a^2 - r^2) \tag{16}$$

The second-order differentiation of Eq. (16) gives:

$$\frac{d^2 w_0(r)}{dr^2} = -\frac{24(1-\mu^2)}{64Eh^3}q_0' \tag{17}$$

Under turning conditions, the deflection $w_0(r)$ produced by the bending moment M_0 due to the residual stress q_0 should be equal to that produced by q_0'. Consequently, equating Eq. (15) with Eq. (17) after rearrangement gives:

$$q_0' = \frac{64h^2}{24(1-\mu^2)}q_0 \tag{18}$$

which will be contributed to q in Eq. (13). Such treatment ignores the variation of residual stress when a turning pass on the machining face has not been fully completed.

3. Simulation Model and Treatment

3.1 High-Order Differential Method for the Simulation Model

A high-order finite-difference method (FDM) [9,10] is used to solve the 2D partial differential equations for the deflection

function w since the FDM is easier to formulate and program than the finite-element method. Let Δ be the step difference between two neighbouring nodes in a finite-difference grid along the neutral plane xoz of the disk shown in Fig. 1. The (x, y)-coordinates of a (i, j)th node in the grid are therefore $(x = i\Delta, y = j\Delta)$. Subsequently, the first-order finite-difference equation for the deflection function $w_{i,j}$ at the (i, j)th node can be expressed as [9]:

$$\left(\frac{\partial w}{\partial x}\right)_{i,j} = \frac{1}{2\Delta}(w_{i+1,j} - w_{i-1,j}),$$

$$\left(\frac{\partial w}{\partial y}\right)_{i,j} = \frac{1}{2\Delta}(w_{i,j-1} - w_{i,j+1}), \ldots \quad (19)$$

While the fourth-order finite-difference equation for the (i, j)th node and its neighbouring nodes in a grid system can be written as:

$$[(w_{i,j+2} - w_{i,j}) + (w_{i,j-2} - w_{i,j}) + (w_{i+2,j} - w_{i,j}) + (w_{i-2,j} - w_{i,j})] + 2[(w_{i+1,j+1} - w_{i,j}) + (w_{i-1,j+1} - w_{i,j}) + (w_{i+1,j-1} - w_{i,j}) + (w_{i-1,j-1} - w_{i,j})] - 8[(w_{i+1,j} - w_{i,j}) + (w_{i-1,j} - w_{i,j}) + (w_{i,j+1} - w_{i,j}) + (w_{i,j-1} - w_{i,j})] = \frac{q_{i,j}\Delta^4}{D} \quad (20)$$

3.2 Treatment of Boundary Condition and Load

Physically, the boundary deflection w around the fixed rim where $x = a \cos\theta$ and $y = a \sin\theta$ (Fig. 1) is zero. That means that $w_{i,j} = 0$ whenever $x^2 + y^2 - a^2 \leq \delta$, where δ is the allowable accuracy. When an (i, j) node is on such a boundary, the deflection w for those fictitious nodes outside the boundary is assumed to be equal to the corresponding nodes either inside or outside the spoke-plate. This implies that $w_{i,j-2} = w_{i,j+2}$, $w_{i,j-1} = w_{i,j+1}$, $w_{i-2,j} = w_{i+2,j}$, $w_{i-1,j} = w_{i+1,j}$, $w_{i-1,j-1} = w_{i+1,j-1}$, and $w_{i-1,j+1} = w_{i+1,j+1}$ in Eq. (20) which itself also becomes zero. Whenever a node is acted on by a concentrated load, the load is assumed to be evenly distributed over its entire area Δ^2 whilst surrounding nodes are allocated an appropriate proportion of the load, depending on their respective distances from the loaded node. For each cutting simulation, the cutting point is always taken as a node where the concentrated load is acting.

3.3 Treatment of Simulation Process

Since the spoke-plate is so thin, the deflection variation in the z-direction (Fig. 1) can be assumed to be negligible. Furthermore, the level of relative deflection on the disk surface to be turned is a maximum along the cutter path. The purpose of this study is to predict the loading condition which allows successful turning to be conducted. Consequently, it is sufficient to achieve the prediction by describing only the neutral plane deflection profile w along the cutter path during the simulation. To further simplify the handling of the data, the feed direction of a cutter is taken along the x-axis (Fig. 1). Under such conditions $\theta = 0$ and the movement of the cutter in the r-direction is always assumed to coincide with the x-axis. Consequently, the deflection of the disk is symmetric to the x-axis and $w_{i,j} = w_{i,-j}$. This leads the finite-difference equation (20) on and about the x-axis to be simplified to:

$$(w_{i+2,0} - w_{i-2,0}) - 8(w_{i+1,0} + w_{i-1,0}) + 4(w_{i+1,1} - w_{i,1,1}) + 20w_{i,0} - 16w_{i,1} + 2w_{i,2} = \frac{q_{i,0}\Delta^4}{D} \quad (21a)$$

where:

$$q_{i,0} = \begin{cases} q_0' + F_y/\Delta^2 & (i = k) \\ q'_0 & (i \neq k) \end{cases} \quad (21b)$$

for a cutter rotating at a rate of n, and fed at a rate of f, to position $r_k = knf\Delta t$ on the cutting surface, at a time $t = k\Delta t$ when the total number of a time steps Δt is k (where $k = 0, 1, 2, \ldots, N$). Figure 2 shows a block diagram of the data processing during the simulation.

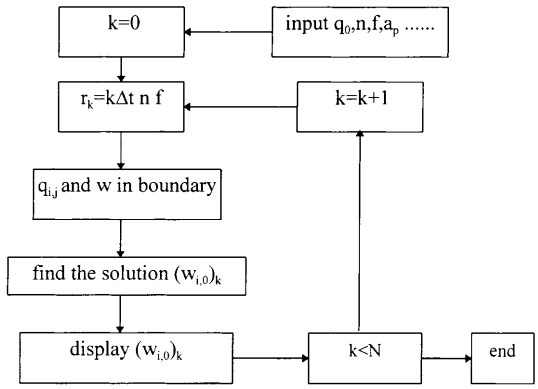

Fig. 2. Basic structure of a simulation computer program.

4. Results and Analysis

Figures 3 to 6 show the simulated deflection results in fine-turning a Ti-6Al-4V thin disk workpiece which had (i) a spoke-radius of 160 mm, and spoke-thickness of 1.5 mm, (ii) coefficient of material $C = 547\ \mathrm{N\,mm^{-2}}$ and cut under the conditions of: cut-depth $a_p = 0.15$ mm, feedrate $f = 0.1\ \mathrm{mm\,rev^{-1}}$, exponent of feedrate $\alpha = 0.64$, tool cutting-edge

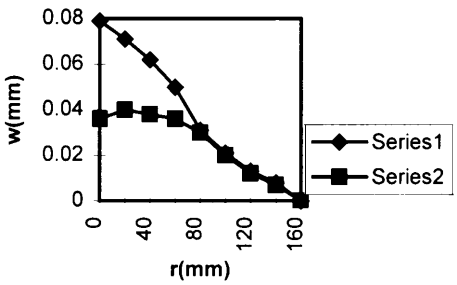

Fig. 3. Predicted deflection distribution when the tool is at $r = 0$ and $r = 70$ mm.

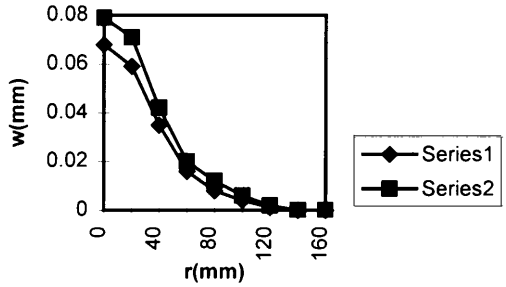

Fig. 4. Distribution of predicted and measured spoke-plate thickness difference after turning.

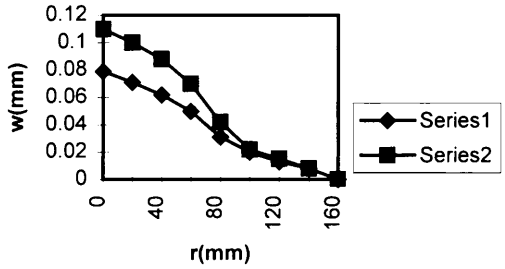

Fig. 5. Similar to Fig. 3, but the cutter travels from the rim towards the centre of the disk.

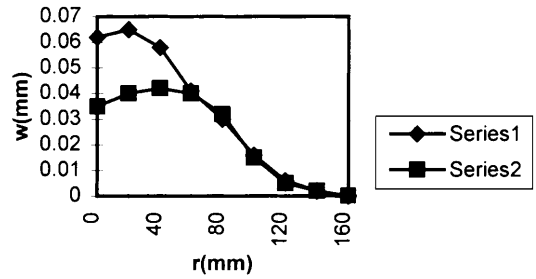

Fig. 6. Similar to Fig. 3, but with the application of a tensional residual stress of 20 N mm^{-2}.

angle $K_r = 90°$, and the constant $K = 0.6$ (see Eq. (14)), with the rotational speed of machine tool $n = 200$ rev min^{-1}.

In Fig. 3, the "series 1" curve illustrates the deflection distribution of the disk along the cutter path when the cutter was at the centre of the disk and just commencing cutting from the centre towards its rim. The "series 2" curve shows the deflection when the disk was being cut from the centre to a position $r = 70$ mm away from the disk centre. It can be observed that the maximum deflection for the first cutting case is at the disk centre and has a magnitude of $w = 0.0792$ mm. Computer simulation showed a symmetric deflection profile with its apex at the disk centre. In the second cutting case, the maximum deflection is 0.04135 mm and occurs at $r = 35$ mm, and gives a skew deflection profile.

Figure 4 shows the distribution of thickness difference of the turned spoke-plate as predicted ("series 2" curve) and measured ("series 1" curve). The predicted values for the "series 2" curve were obtained from the maximum value of the individual deflection simulation curves when the cutter was at a number of different positions at and between $0 \leq r \leq 160$ mm. Results show that the predicted thickness difference is higher than the actual measurements. This suggests that the residual tolerance is looser than the actual one. Subsequently, when the predicted deflection gives a value equal to the required machining tolerance, it produces a tighter tolerance than the expected one. The maximum thickness difference of the simulated value is almost 19% higher than the experimental value, and the difference between the prediction and measurement tends to reduce from the centre towards the rim.

The cutting direction also influences the deflection distribution along the axis of its direction of cut. Results for a cutter travelling from the rim of the spoke-plate to its centre are shown in Fig. 5. It can be seen that the maximum deflection increases to 0.1107 mm when the cutter arrives at the centre ("series 2" curve – Fig. 5) and the general deflection profile is larger in comparison with its counterpart when the cutter is travelling from the centre to the rim (Fig. 3). Similarly, the maximum deflection for the cutter at $r = 70$ mm is approximately equal to 0.08 mm and occurs at the disk centre ("series 1" curve – Fig. 5) instead of skewing 35 mm away from centre as shown in Fig. 3. Such characteristics are because the flexural rigidity in the outer machined annular area of the disk was reduced when turning from the outer rim towards the inner part. This implies that turning from the centre towards the outer rim is a better way to achieve finer machining tolerances.

Deflection simulation with a tensional residual stress $q_0 = 20$ N mm^{-2}, uniformly applied to the disk which was being cut from the centre to the rim, with the position of the cutter at $r = 70$ mm, is shown in Fig. 6. It should be noted that the "series 1" curve presents the deflection distribution when residual stress was not considered while the "series 2" curve depicts that when tensional residual stress was taken into account. The "series 1" curve shows that the maximum deflection is approximately 0.065 mm and shifted slightly away from the disk centre to $r \approx 20$ mm, whilst the "series 2" case has a maximum of 0.04135 mm and is at $r \approx 40$ mm. Comparing the two curves, it can also be seen that deflection for the two cases is almost the same when $r > 60$ mm. For the region of $r \leq 60$ mm, the deflection for the case under tensional residual stress is generally higher than the case with only the cutting load. Such characteristics seem to suggest that the increase in tensional residual stress reduces the degree of skewing, but increases relatively the deflection and improves the relative symmetry. A deduction can also be drawn from this study that the application of compressive residual stress would generally diminish the deflection and produce higher accuracy and successful machining.

Normally, the larger the cutting depth a_p and feedrate f, and the smaller the K_r, the larger is the concentrated load and the higher is the asymmetry of the deflection.

4. Conclusion

The theory of small deflection of sheet-disk bending is suitable for use for the physical simulation of turning a thin disk-shaped workpiece. Such a simulation enables the estimation of the loosest tolerance that the turning would produce, and subsequently allows the determination of whether a specific

finishing thickness cut of thin disk-shaped workpiece can be achieved successfully for a particular machining condition. The application of the technique can also predict the machining condition appropriate for achieving a particular specification of a thin disk-shaped workpiece so as to optimise the operation and reduce costs. Simulation results also show that turning a sheet spoke-plate from the disk centre to the rim boundary reduces the magnitude of deflection, thus producing more accurate machining. Consequently, this is a relatively better turning method to use when the spoke-plate is thin.

References

1. H. El-Mounayri, M. A. Elbestawi, A. D. Spence and S. Bedi, "General geometric modelling approach for machining process simulation", International Journal of Advanced Manufacturing Technology, 13(4), pp. 237–247, 1997.
2. E. A. Gani, J. P. Kruth, P. Vanherck and B. Lauwers, "A geometrical model of the cut in five-axis milling accounting for the influence of tool orientation", International Journal of Advanced Manufacturing Technologies, 13(10), pp. 677–684, 1997.
3. E. J. A. Armarego and N. P. Desphande, "Computerized end milling force prediction with cutting models allowing for eccentricity and cutter deflection", Annals CIRP, 40(1), pp. 35–38, 1991.
4. P. Atherton, C. Earl and C. Fred, "A graphical simulation system for dynamic five axis NC verification", Society of Manufacturing Engineers, Autofaxt Show, Detroit, USA, pp. 2.1–2.12, November 1987.
5. R. B. Jerrard, R. L. Drysda, K. Hauck, "Geometric simulation for numerical control machining", Proceedings ASME International Computers in Engineering Conference, San Francisco, 2, pp. 129–136, 31 July–3 August, 1988.
6. S. Takata, M. D. Tsai and T. Sata, "A cutting simulation system for machinability evaluation using a workpiece model", Annals CIRP, 38(1), pp. 417–420, 1989.
7. Yong Fang and F. W. Liou, "Visual Prototyping of Mechanical Assemblies with Deformable Components", Journal of Manufacturing Systems, 16(3), pp. 211–219, 1997.
8. Huang Zhaisheng, Elastics and its Applications, Zhejiang University Press, China, 1980.
9. Huang Yan, Elastic Shell Theory, Defense Science and Technology Press, China, 1982.
10. Liu Fangwen, Shell Theory, Zhejiang University Press, China, 1986.
11. Zhang Youzhen, Metal Cutting Theory, Aeronautical Industry Press, China, 1985.